

Lu, Hongfang; Ma, Guoguang; Cao, Lianjin; Azimi, Mohammadamin

## Article

# Optimization of light hydrocarbon recovery system in condensate gas field

Energy Reports

## Provided in Cooperation with:

Elsevier

*Suggested Citation:* Lu, Hongfang; Ma, Guoguang; Cao, Lianjin; Azimi, Mohammadamin (2019) : Optimization of light hydrocarbon recovery system in condensate gas field, Energy Reports, ISSN 2352-4847, Elsevier, Amsterdam, Vol. 5, pp. 1209-1221, <https://doi.org/10.1016/j.egy.2019.08.021>

This Version is available at:

<https://hdl.handle.net/10419/243663>

### Standard-Nutzungsbedingungen:

Die Dokumente auf EconStor dürfen zu eigenen wissenschaftlichen Zwecken und zum Privatgebrauch gespeichert und kopiert werden.

Sie dürfen die Dokumente nicht für öffentliche oder kommerzielle Zwecke vervielfältigen, öffentlich ausstellen, öffentlich zugänglich machen, vertreiben oder anderweitig nutzen.

Sofern die Verfasser die Dokumente unter Open-Content-Lizenzen (insbesondere CC-Lizenzen) zur Verfügung gestellt haben sollten, gelten abweichend von diesen Nutzungsbedingungen die in der dort genannten Lizenz gewährten Nutzungsrechte.

### Terms of use:

*Documents in EconStor may be saved and copied for your personal and scholarly purposes.*

*You are not to copy documents for public or commercial purposes, to exhibit the documents publicly, to make them publicly available on the internet, or to distribute or otherwise use the documents in public.*

*If the documents have been made available under an Open Content Licence (especially Creative Commons Licences), you may exercise further usage rights as specified in the indicated licence.*



<https://creativecommons.org/licenses/by-nc-nd/4.0/>



## Research paper

# Optimization of light hydrocarbon recovery system in condensate gas field



Hongfang Lu<sup>a,b</sup>, Guoguang Ma<sup>a,\*</sup>, Lianjin Cao<sup>a</sup>, Mohammadamin Azimi<sup>b</sup>

<sup>a</sup> State Key Laboratory of Oil and Gas Reservoir Geology and Exploitation, Southwest Petroleum University, Chengdu 610500, China

<sup>b</sup> Trenchless Technology Center, Louisiana Tech University, Ruston LA 71270, United States

## ARTICLE INFO

## Article history:

Received 12 February 2019

Received in revised form 6 July 2019

Accepted 19 August 2019

Available online xxxx

## Keywords:

Light hydrocarbon recovery

Condensate field

Sequential-modular method

Exergy loss

Black box model

Direct heat exchange

## ABSTRACT

During the middle and later stages of condensate gas field development, the flow rate and pressure of the light hydrocarbon recovery system gradually decrease, and there is a certain deviation between the design parameters and the actual operation parameters of the equipment, resulting in a decrease in the recovery rates of propane ( $C_3$ ) and higher hydrocarbons ( $C_{3+}$ ). Therefore, it is necessary to optimize the system to obtain greater economic value. In order to solve this problem, the paper analyzes the sensitivity of the equipment operating parameters based on the sequential-modular method. The black box model is used to analyze the equipment and the whole system, and the subsystem with large exergy loss is found. Moreover, this paper optimizes the light hydrocarbon recovery system using parameter optimization and process optimization, and compares the results. According to the analysis, the main conclusions are drawn: (1) The outlet pressure of expander and the temperature of deethanizer bottom have great influence on the light hydrocarbon recovery system, the reduction of the expander outlet pressure from 2.3 MPa to 1.8 MPa can increase the recovery of  $C_3$  by 5%. Decreasing the bottom temperature of the deethanizer from 80 °C by 20 °C can increase the recovery of  $C_3$  by 9.2%. (2) Optimized process using direct heat exchange technology has a better optimization effect than the parameter optimization process, the  $C_3$  recovery of the optimized system increased by 19.1% to 93%, the recovery of  $C_{3+}$  increased by 14.4% to 95%.

© 2019 The Authors. Published by Elsevier Ltd. This is an open access article under the CC BY-NC-ND license (<http://creativecommons.org/licenses/by-nc-nd/4.0/>).

## 1. Introduction

As a relatively clean energy source, natural gas has become more and more widely used (Lu et al., 2019a,b; Ma et al., 2019). Therefore, improving natural gas utilization is currently a hot spot. In the middle and later stages of development of some gas fields, the recovery rates of  $C_3$  and  $C_{3+}$  in the system are reduced due to the decrease in the treatment volume and pressure, thus failing to meet the system design requirements. Taking DLB gas field as an example, the designed processing capacity is  $25 \times 10^4$   $Nm^3/d$ , and the turn-down ratio is  $\pm 20\%$ . However, the current gas processing capacity is only  $16 \times 10^4$   $Nm^3/d$ , the recovery rates of  $C_3$  and  $C_{3+}$  have been reduced accordingly. On the one hand, improving the recovery rate of light hydrocarbons can ensure the quality of commercial gas, on the other hand, it can also reduce pollution and improve economic benefits. Therefore, in this paper, the main target is to use the process simulation method to

analyze the light hydrocarbon recovery system and put forward the optimization scheme.

At present, the more mature condensate recovery processes includes DHX process, light oil reflux process, membrane separation process, and GSP. These processes aim at improving the recovery rate of light hydrocarbons and saving energy consumption (Zhao, 2013). DHX technology was first proposed by Esso Resources Canada in 1984. The technology is an improvement in the expansion refrigeration process, which is to add an absorber tower between the expander and deethanizer. In order to improve the recovery rate, if we want to reform the traditional expansion refrigeration process, the DHX technology is often used. Under the same conditions, the recovery rate of  $C_3$  can be increased from 72% to 95%, and the investment cost for retrofitting is lower (Limb and Czarnecki, 1987; Khan, 1985; Aggarwal and Singh, 2001). In recent years, membrane separation technology in the gas separation process has been greatly developed, the technology has good economic returns and good adaptability. According to the different materials, the material needed for membrane separation technology is divided into the porous membrane and non-porous membrane, and the principle of penetration is different. Currently, non-porous membranes are widely used in light hydrocarbon recovery processes and are

\* Correspondence to: State Key Laboratory of Oil and Gas Reservoir Geology and Exploitation, Southwest Petroleum University, No. 8 Xindu road, Xindu District, Chengdu 610500, China.

E-mail addresses: [luhongfang\\_sci@126.com](mailto:luhongfang_sci@126.com) (H. Lu), [mgg@swpu.edu.cn](mailto:mgg@swpu.edu.cn) (G. Ma).

**Nomenclature**

$C_3$	Propane
$C_{3+}$	Hydrocarbons with more than three carbon atoms
$P$	Pressure, MPa
$v$	Molar volume, $m^3/kmol$
$T$	Temperature, $^{\circ}C$
$R$	Molar gas constant, $8.314 \text{ kJ}/(\text{kmol } ^{\circ}C)$
$a, b$ and $\alpha$	Coefficient of state equation
$\omega$	Acentric factor
$r$	Reduced state
$P_c$	Critical pressure of the system, MPa
$T_c$	Critical temperature of the system, $^{\circ}C$
$T_r$	Reduced temperature
$\rho$	Molar density, $kmol/m^3$
$A_i, B_i, C_i, D_i, E_i, F_i, G_i$	Thermodynamic constants of component $i$
$E_{xim}$	Import exergy
$E_{xlr}$	Internal exergy
$E_{xlf}$	External exergy
$E_{xout}$	Output exergy
$e_{xm}$	Exergy of unit material flow, $kg/h$
$h$	Enthalpy of unit material flow in the current system, $kJ/kg$
$h_0$	Enthalpy of unit material flow in the reference state, $kJ/kg$
$T_0$	Reference temperature, $^{\circ}C$
$s$	Entropy of unit material flow in the current system, $kJ/kg \text{ } ^{\circ}C$
$s_0$	Entropy of unit material flow in the reference state, $kJ/kg \text{ } ^{\circ}C$
$E_{xm}$	Exergy of material flow, $kg/h$
$m$	Mass of material flow, $kg$
$\Sigma E^+$	Total exergy of material flow (or energy flow) entering the system, $kJ/h$
$\Sigma E^-$	Total exergy of material flow (or energy flow) exiting the system, $kJ/h$
$F_i$	Flow rate of material flow $i$ , $kmol/h$
$x_{i,j}$	Mole fraction of $j$ in material flow $i$
$K_j$	Gas–liquid equilibrium constant for component $j$
$Q$	Total heat load, $kJ/h$
$Q_i$	Heat obtained by the cold flow $i$ , $kJ/h$
$A_i$	Heat transfer area, $m^2$
$K_i$	Heat transfer coefficient of cold flow and heat flow, $kW/m^2 \text{ } ^{\circ}C$
$\Delta t_{mi}$	Logarithmic mean temperature difference between the cold flow and the heat flow, $^{\circ}C$
$H_6, H_7$	Import enthalpy and outlet enthalpy of hot fluid, $kJ/h$
$H_{18}, H_{19}$	Inlet enthalpy and outlet enthalpy of the first cold flow, $kJ/h$
$H_{20}, H_{23}$	Inlet enthalpy and outlet enthalpy of the second cold flow, $kJ/h$
$S_8, S_9$	Entropies before expansion and after expansion, $kJ/kmol \text{ } ^{\circ}C$
$T_8, T_9$	Temperatures before expansion and after expansion, $^{\circ}C$
$P_8, P_9$	Pressures before expansion and after expansion, MPa

$H_8, H_9$	Enthalpies before expansion and after expansion, $kJ/kmol$ ;
$W, W_s$	Actual work and ideal work during expansion process, $kJ/kmol$
$\eta_s$	Adiabatic efficiency; $k$ is adiabatic index
$T_{23}, T_{24}$	Suction temperature and exhaust temperature of compressor, $^{\circ}C$
$P_{23}, P_{24}$	Suction pressure and exhaust pressure of compressor, MPa
$k$	Adiabatic index of compressed gas; $\varepsilon$ is compression ratio
$V$	Amount of gas, $kmol/h$
$L$	Amount of liquid, $kmol/h$
$z_i$	Mole fraction of component $i$ in law gas
$x, y$	Mole fraction
$h, H$	Enthalpy, $kJ/kmol$
$Q$	Heat load, $kJ/h$
$E_i$	Energy consumption of each unit in the equipment, $kJ/h$
$F_{C3+}$	Flow rate of $C_{3+}$ in the recovered light hydrocarbons, $kmol/h$
$\Delta t$	Minimum temperature difference of heat exchanger, $^{\circ}C$
$F_{C2-}$	Molar flow of $C_1$ and $C_2$ in the recovered light hydrocarbon, $kmol/h$
$F_{C5+}$	The molar flow of $C_{5+}$ , $kmol/h$
$F_{LPG}$	Molar flow of LPG, $kmol/h$
$P$	Outlet pressure of expander, MPa
$T$	Temperature of deethanizer bottom, $^{\circ}C$
$P_1$	Pressure of liquefied gas tower bottom, MPa
$T_1$	Temperature of reboiler (liquefied gas tower bottom), $^{\circ}C$
$P_c$	Critical pressure, MPa
$T_c$	Critical temperature, $^{\circ}C$

**Abbreviations**

DLB	Dalaoba, a name of a gas field in Xinjiang, China
DHX	Direct heat exchange
GSP	Gas subcooled process
LSP	Liquid subcooled process
RSV	Recycle split-vapor
RR	Residue recycle process
PSA	Pressure swing adsorption
LPG	Liquefied petroleum gas
PR	Peng–Robinson
SQP	Successive quadratic programming

separated according to the principle of dissolution and diffusion (Shin et al., 1992; Fernandes et al., 2000). GSP is based on the improvement of lean natural gas ( $C_{2+} < 100 \text{ mL}/m^3$ ) processing plants, the technology can not only make the  $C_2$  recovery rate high, but also allow the content of  $CO_2$  in natural gas to be higher than that of in the expansion refrigeration process, and the power consumption is lower (Wilkinson and Hudson, 1982). Unlike the GSP process, the LSP is based on the improvement of rich natural gas processing plants. The process not only reduces the low temperature and high-pressure part of the conventional process, but also saves energy consumption. This process can

treat gas with high CO<sub>2</sub> content (Pitman et al., 1998). RSV process is a process that can obtain higher recovery rate (above 98%) of ethane. This process combines the characteristics of GSP and RR technology. Unlike the GSP, the top of the demethane tower has a compression and condensing unit. This process is suitable for the recovery process of light hydrocarbon which is rich in CO<sub>2</sub>, and it can prevent the occurrence of ice blocking when the natural gas is treated at low temperature (Baker et al., 1998). Vortex tube refrigeration process is suitable for low pressure natural gas, which is generally 0.9–1.5 MPa. This method is commonly used for condensate recovery in remote gas fields (Lyu and Zhang, 2010). Light oil reflux process is based on the principle of oil absorption, which can increase the recovery rate of condensate. This process is suitable for low pressure shallow cooling device at about −35 °C (Zhao, 2003). PSA technology has been developed in 1980s. So far, the technology has been widely applied. PSA has a good effect in gas separation. In the process of light hydrocarbon recovery, the pretreated gas is absorbed by the adsorption bed, which absorbs the components with higher boiling point than propane, thus achieving the effect of the separation of light hydrocarbons (Chan et al., 1981).

From the perspective of gas separation technology, there are three most widely used technologies: oil-absorption process, adsorption method, and condensation separation method. Compared with other light hydrocarbon recovery methods, the condensation separation method has the advantages of high recovery efficiency, low investment and low operation cost. It has gradually replaced the oil-absorption process and adsorption method after 1970s (Liu and Wang, 2000). According to the different ways to provide cold energy, condensation separation method can be divided into refrigerant refrigeration method, expansion refrigeration method and combined refrigeration method.

Refrigerant refrigeration method belongs to shallow cooling method, it needs to set up independent refrigeration system in external. The cooling capacity of this method is not directly related to the natural gas to be separated, and there is no requirement for the quality and pressure of the raw gas. The cooling capacity can be adjusted according to the gas volume, the quality of the raw gas and the refrigeration temperature. This method is suitable for the raw gas which the composition is relatively rich (Krasae-In et al., 2010). The expansion refrigeration method relies on the pressure difference between raw gas and commercial gas to provide cold energy. Due to the low refrigeration temperature and the high condensing pressure of the expander, the C<sub>3+</sub> recovery rate is relatively high. This method is applicable to gas fields with relatively stable gas quantity and pressure, relatively poor gas composition and high condensate recovery requirements (Chaiwongsa and Wongwises, 2008). The combined refrigeration method belongs to the sub-cryogenic cooling method, the cold energy is provided by the expansion refrigeration method and refrigerant method. The advantages of the combined refrigeration method are good adaptability, high recovery rate of C<sub>2</sub> and low energy consumption of the equipment. Generally, the refrigeration temperature of this process is from −80 °C to −100 °C, and the recovery rate of C<sub>3</sub> is in the range of 75%–85% (Wang, 2003).

From the aspect of light hydrocarbon recovery process optimization, the focus of the study is to improve the recovery rate of light hydrocarbon and reduce the energy consumption. The main methods are: (1) Optimization of equipment operating parameters; (2) Increase the rate of gas treatment; (3) Change the mode of refrigeration; (4) New technology for recovery of light hydrocarbons; (5) Use of efficient equipment (Wu, 2013; Cao, 2015).

This paper optimizes the light hydrocarbon recovery system of DLB condensate gas field using two different ways: parameter optimization and process optimization, and compares various

indicators to determine the final scheme. Different from other scholars' research, the optimization target of this paper is not only considering the light hydrocarbon recovery, but also considering the energy consumption of the system. The rest of the paper is organized as follows: Section 2 describes the problems of light hydrocarbon recovery system in DLB gas field, Section 3 introduces the basic theory used in this paper, Section 4 describes the process of parameter optimization and mathematical model, Section 5 shows simulation results, Section 6 shows two methods of light hydrocarbon optimization and comparison results.

## 2. Problem description

As shown in Fig. 1, in DLB condensate gas field, high-pressure raw gas enters the separator (free water, oil droplets, and dust are removed). Then the gas enters molecular sieve drying unit and mercury removal unit, saturated water, and a small amount of mercury in natural gas are removed. The gas from the mercury removal unit is cooled down in a cold box and then enters a cryogenic separator to remove the condensed heavy components. The gas from the cryogenic separator enters the turboexpander for expansion and cooling, and then enters deethanizer from the top. The liquid phase at the bottom of the cryogenic separator is used as the feed of the deethanizer after the heat exchange of the cold box. The dry gas from the top of the deethanizer is reheated by the cold box heat exchanger and enters the pressurize section of the expander to be taken as commercial gas and to be exported. The liquid hydrocarbons at the bottom of the deethanizer tower enter the liquefied gas tower by differential pressure, and the LPG and light oil products are produced.

The actual operating parameters and design parameters of the light hydrocarbon recovery unit are shown in Table 1. It can be seen from Table 1 that there is a certain deviation between the operating values and the designed values.

According to the design requirements of light hydrocarbon recovery system, the recovery rate of C<sub>3</sub> should not be less than 78%, and the recovery rate of C<sub>3+</sub> should not be less than 82%. However, the recovery of C<sub>3</sub> and C<sub>3+</sub> are reduced due to the decrease of treatment volume and inlet pressure, the change of the content of the raw gas and the operation parameters of the equipment. According to the current field data, the recovery rate of C<sub>3</sub> is 73.9%, and the recovery rate of C<sub>3+</sub> is 80.6%. Both of them have not reached the designed requirements. Therefore, it is necessary to optimize the light hydrocarbon recovery equipment.

## 3. Basic theory

### 3.1. State equation

The objective of this study is the light hydrocarbon recovery system. The PR equation can accurately calculate the molar volume and thermodynamic properties of liquid phase. Therefore, the PR equation is used to calculate the gas-liquid equilibrium. This equation is also widely applied in natural gas treatment (Patel and Teja, 1982; Cismondi and Mollerup, 2005).

The expression of the PR equation is:

$$P = \frac{RT}{v-b} - \frac{a}{v(v+b) + b(v-b)} \quad (1)$$

where:

$$b = 0.0778 \frac{RT_c}{P_c} \quad (2)$$

$$a = a(T_c) \alpha \quad (3)$$

$$a(T_c) = 0.45727 \frac{R^2 T_r^2}{P_c} \quad (4)$$

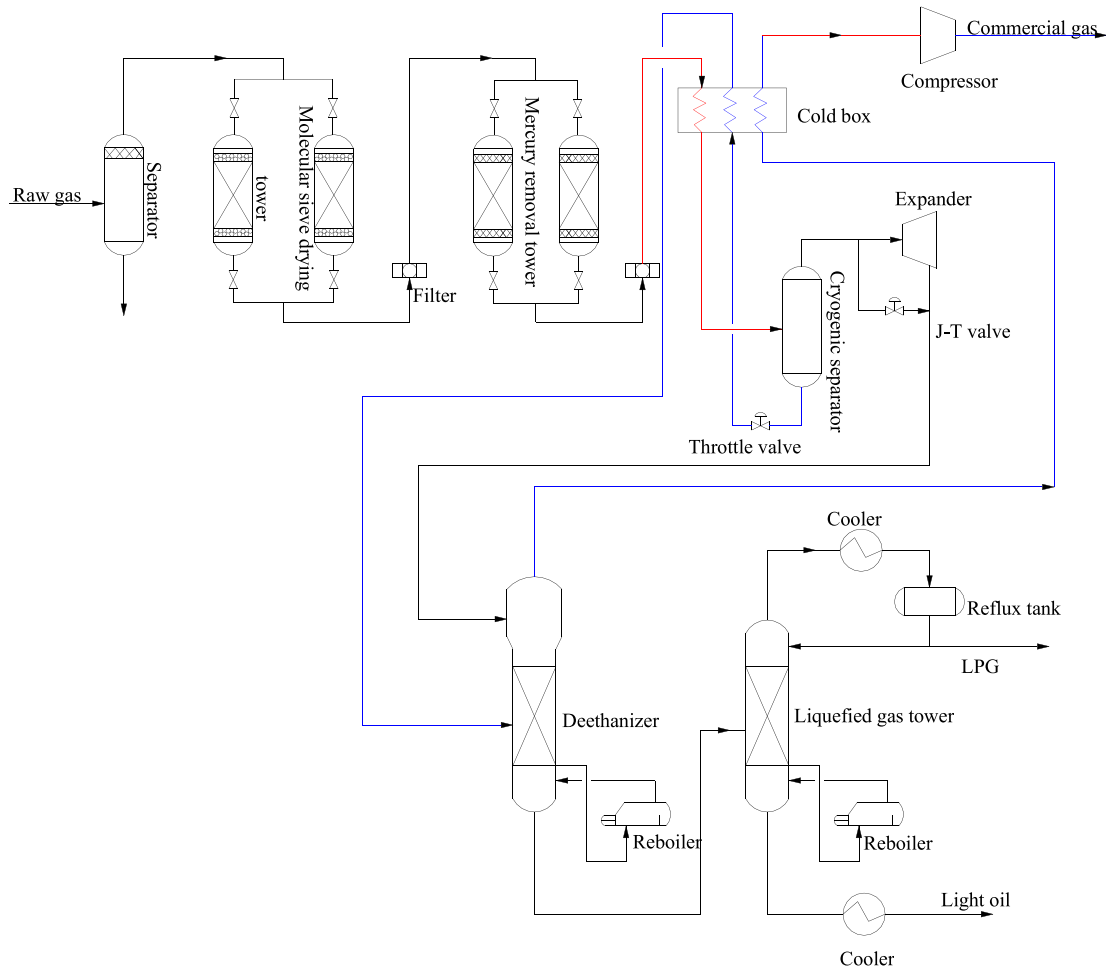


Fig. 1. Process flow diagram of light hydrocarbon recovery system in DLB condensate gas field.

Table 1

Actual operating parameters and design parameters of the system.

Equipment	Actual operating parameters		Designed parameters	
	Pressure (MPa)	Temperature (°C)	Pressure (MPa)	Temperature (°C)
Separator	6.03	33.0	8.50	26.3
Molecular sieve drying tower	6.00	33.0	8.4	26.0
Mercury removal tower	5.99	33.0	8.4	26.0
Cryogenic separator (gaseous phase)	5.96	−33.0	8.39	−23.0
Cryogenic separator (liquid phase)	5.96	−33.0	8.39	−21.0
Export of throttle valve	2.21	−55.0	2.58	−48.9
Expander (Expansion section)	2.20	−69.1	2.20	−76.8
Expander (Pressurize section)	2.54	42.7	2.61	45.4
Deethanizer	Top	2.20	2.11	−66.2
	Bottom	2.20	2.15	89.9
Liquefied gas tower	Top	1.20	1.30	45.0
	Bottom	1.20	1.33	170.0

$$\alpha = [1 + (0.37464 + 1.5422\omega - 0.26992\omega^2)(1 - T_r^{0.5})]^2 \quad (5)$$

$$T_r = \frac{T}{T_c} \quad (6)$$

### 3.2. Thermodynamic calculation formula

Many calculations of thermodynamic properties, such as enthalpy, entropy, fugacity, fugacity coefficient, etc., are used in the light hydrocarbon recovery unit model and these can be derived from the PR state equation.

The formula of isothermal enthalpy difference is:

$$H - H_0 = \frac{P}{\rho} - RT + L_1 \frac{[(f_w + 1)(f_w \sqrt{T_r} - f_w - 1)]}{b} \ln \frac{1 + 2.414b\rho}{1 - 0.414b\rho} \quad (7)$$

where:

$$f_w = 0.37464 + 1.54226\omega - 0.26992\omega^2 \quad (8)$$

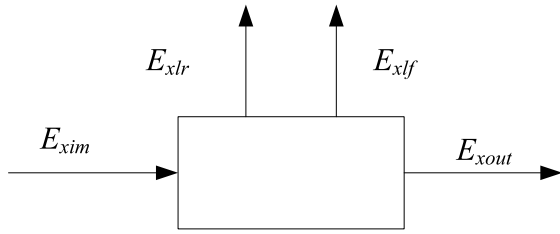


Fig. 2. Black box model diagram.

$$L_1 = 0.457235 \frac{R^2 T_c^2}{P_c} \quad (9)$$

$$H^0 = \sum y_i H_i^0 \quad (10)$$

$$H_i^0 = A_i + B_i T + C_i T^2 + D_i T^3 + E_i T^4 + F_i T^5 \quad (11)$$

The formula of isotherm entropy difference:

$$S - S_0 = -R \ln \left( \frac{\rho RT}{101.325} \right) - R \ln (1 - b\rho) + \frac{L_1}{b} \left( \frac{f_w^2}{T_c} - \frac{f_w (f_w + 1)}{\sqrt{TT_c}} \right) \ln \frac{1 + 2.414b\rho}{1 - 0.414b\rho} \quad (12)$$

$$S^0 = \sum_i y_i S_i^0 + y_i \ln y_i \quad (13)$$

$$S_i^0 = B_i \ln T + 2C_i T + \frac{3}{2} D_i T^2 + \frac{4}{3} E_i T^3 + \frac{5}{4} F_i T^4 + G_i \quad (14)$$

### 3.3. Exergy analysis model

In engineering, the black box model is usually used for exergy analysis, as shown in Fig. 2. The black box model can obtain exergy, effective exergy and exergy loss by inputting exergy of material flow or energy flow of input and output systems (Morosuk and Tsatsaronis, 2008; Cheng et al., 2017). The model ignores the internal specific conditions of the system, and the calculation process is simple, as shown in Fig. 2.

### 3.4. Calculation of exergy

The calculation formula for exergy is:

$$e_{xm} = h - h_0 - T_0 (s - s_0) \quad (15)$$

$$E_{xm} = e_{xm} m \quad (16)$$

### 3.5. Exergy loss

Exergy loss analysis also uses black box model, the expression of exergy loss is:

$$D_x = \sum E^+ - \sum E^- \quad (17)$$

The expression of exergy efficiency is:

$$\eta_E = \frac{\sum E^-}{\sum E^+} \quad (18)$$

### 3.6. Sequential-modular method

Sequential-modular method refers to the use of sequential calculation method of unit module to solve the system model, and the unit module is the basic unit of calculation. The solving process of sequential-module method is as follows Hillestad and Hertzberg (1986):

- (1) Conversion of a system process diagram into a structural unit diagram composed of nodes and streams;
- (2) Identify the indivisible subsystem of the process system through system analysis and assign the order of solution to each subsystem;
- (3) Break the indivisible subsystem, determine the best fracture flow, and set the convergence unit;
- (4) Calculate the order of each node in the subsystem containing the loop;
- (5) Solve the entire system in the order of subsystems and nodes.

### 4. Case study

Based on the solving process of sequential-modular method, this paper takes the hydrocarbon recovery system in DLB condensate gas field as a case study, the structural unit diagram of this system can be seen in Fig. 3.

The light hydrocarbon recovery system of DLB condensate field is mainly divided into two main subsystems, which are the purification system and the refrigeration fractionation system. The identification, sorting and fracture of the inseparable subsystem are shown as follows:

#### (a) Purification system

The purification system mainly includes drying and mercury removal of raw material gas. The system does not contain loops. It only needs to identify and sort out the indivisible subsystem of the structural unit diagram.

Recognition and sorting of inseparable subsystems by adjacency matrices:

$$\begin{bmatrix} 0 & 1 & 0 & 0 & 0 \\ 0 & 0 & 1 & 0 & 0 \\ 0 & 0 & 0 & 1 & 0 \\ 0 & 0 & 0 & 0 & 1 \\ 0 & 0 & 0 & 0 & 0 \end{bmatrix} \Rightarrow \begin{bmatrix} 0 & 1 & 0 & 0 \\ 0 & 0 & 1 & 0 \\ 0 & 0 & 0 & 1 \\ 0 & 0 & 0 & 0 \end{bmatrix} \\ \Rightarrow \begin{bmatrix} 0 & 1 & 0 \\ 0 & 0 & 1 \\ 0 & 0 & 0 \end{bmatrix} \Rightarrow \begin{bmatrix} 0 & 1 \\ 0 & 0 \end{bmatrix} \Rightarrow [0]$$

Therefore, the solution sequence is  $A_1 \rightarrow A_2 \rightarrow A_3 \rightarrow A_4 \rightarrow A_5$ .

#### (2) Refrigeration fractionation system

The structural unit diagram of refrigeration fractionation system can be seen in Fig. 3. Its adjacency matrix is:

$$\begin{bmatrix} 0 & 1 & 0 & 0 & 1 & 0 & 1 \\ 1 & 0 & 1 & 0 & 0 & 0 & 0 \\ 0 & 0 & 0 & 1 & 0 & 0 & 0 \\ 1 & 0 & 0 & 0 & 1 & 0 & 0 \\ 0 & 0 & 0 & 1 & 0 & 1 & 0 \\ 0 & 0 & 0 & 0 & 0 & 0 & 0 \\ 0 & 0 & 0 & 0 & 0 & 0 & 0 \end{bmatrix} \Rightarrow \begin{bmatrix} 0 & 1 & 0 & 0 & 1 & 0 \\ 1 & 0 & 1 & 0 & 0 & 0 \\ 0 & 0 & 0 & 1 & 0 & 0 \\ 1 & 0 & 0 & 0 & 1 & 0 \\ 0 & 0 & 0 & 1 & 0 & 1 \\ 0 & 0 & 0 & 0 & 0 & 0 \end{bmatrix} \\ \Rightarrow \begin{bmatrix} 0 & 1 & 0 & 0 & 1 \\ 1 & 0 & 1 & 0 & 0 \\ 0 & 0 & 0 & 1 & 0 \\ 1 & 0 & 0 & 0 & 1 \\ 0 & 0 & 0 & 1 & 0 \end{bmatrix}$$

The loop A6-A7-A6 is found by using path search method, and the virtual node L1 is used instead of the loop node, the new adjacency matrix can be obtained. The loop L1-A8-A9-L1 is found

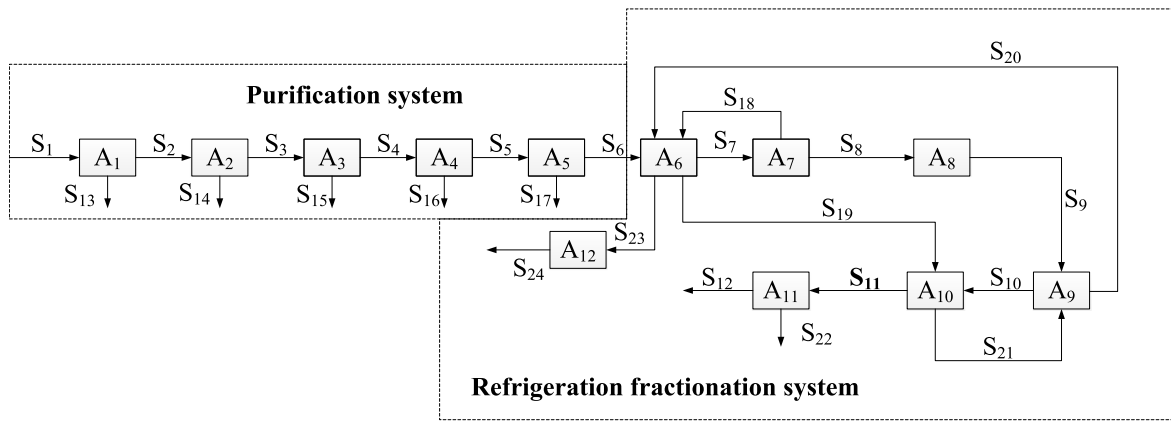


Fig. 3. Structural unit diagram of hydrocarbon recovery system in DLB condensate gas field.

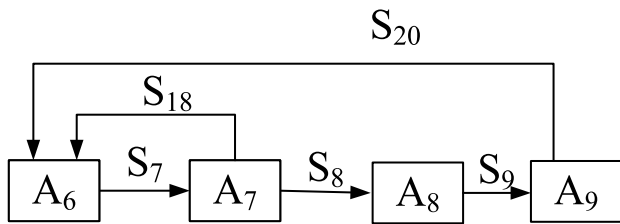


Fig. 4. Inseparable subsystem with loops.

by analogy, and the new adjacency matrix is obtained by using the virtual node L2 instead of the loop node. The new adjacency matrix is:

$$\begin{bmatrix} 0 & 1 & 0 & 0 & 1 \\ 1 & 0 & 1 & 0 & 0 \\ 0 & 0 & 0 & 1 & 0 \\ 1 & 0 & 0 & 0 & 1 \\ 0 & 0 & 0 & 1 & 0 \end{bmatrix} \Rightarrow \begin{bmatrix} 0 & 0 & 1 & 0 \\ 1 & 0 & 1 & 0 \\ 0 & 0 & 0 & 1 \\ 1 & 0 & 1 & 0 \end{bmatrix} \Rightarrow \begin{bmatrix} 0 & 1 \\ 0 & 0 \end{bmatrix}$$

Therefore, the sequence of the refrigeration fractionation system is: (A6-A7-A8-A9)→A10→A11→A12.

(3) Break inseparable subsystem using loop matrix

The inseparable subsystem with loops is shown in Fig. 4. Simple circuits L1 and L2 are shown in Fig. 5.

The loop matrix is:

$$L_1 \begin{bmatrix} 1 & 0 & 0 & 1 & 0 \\ 1 & 1 & 1 & 0 & 1 \end{bmatrix}$$

$$\rho \begin{bmatrix} 2 & 1 & 1 & 1 & 1 \end{bmatrix}$$

It can be obtained from loop analysis that  $S_8 \subset S_7$ ,  $S_9 \subset S_7$ ,  $S_{18} \subset S_7$ ,  $S_{20} \subset S_7$ , it means that S8, S9, S18, and S20 are not independent columns. Therefore, S7 is considered to be a flow broken line. Therefore, the order of solving the structural unit of the whole light hydrocarbon recovery system is  $A_1 \rightarrow A_2 \rightarrow A_3 \rightarrow A_4 \rightarrow A_5 \rightarrow (A_6-A_7-A_8-A_9) \rightarrow A_{10} \rightarrow A_{11} \rightarrow A_{12}$ .

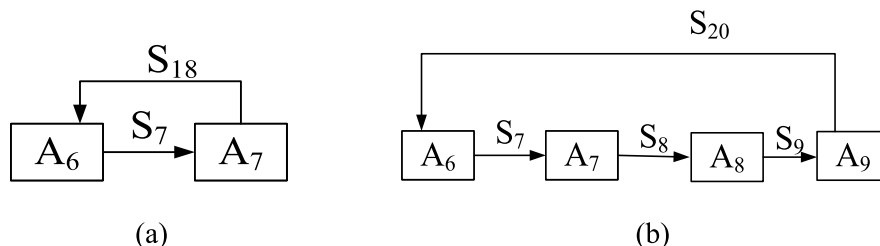


Fig. 5. Simple circuit: (a) L1 circuit; (b) L2 circuit.

The light hydrocarbon recovery system in DLB condensate gas field consists of several subsystems, including separation system, gas drying system, refrigeration system, heat exchange system, fractionation system and so on. The entire system has twelve unit processes, and the types of unit modules involved in the simulation include separators, heat exchangers, turbine expanders, compressors and rectification tower. Mathematical models of equipment are shown in Appendix.

## 5. Results

### 5.1. Effect of condensing pressure and condensing temperature

Sequential-modular method is used to optimize the parameters of light hydrocarbon recovery system in DLB condensate field, the factors that affect the recovery rate of the system should be found. The light hydrocarbon recovery system uses the condensation separation method, so the condensing temperature and condensing pressure are the main factors affecting the recovery rate. The liquefaction rate of each component varies with temperature as shown in Fig. 6 (5.0 MPa) and Fig. 7 (6.0 MPa).

It can be seen from Figs. 6 and 7, lowering the condensing temperature and increasing the condensing pressure can increase the liquefaction rates of C<sub>3</sub> and C<sub>3+</sub>. With the decrease of condensing temperature and the increase of condensing pressure, the increase rate of liquefaction rate of C<sub>3</sub> and C<sub>3+</sub> decreases, while the liquefaction rate of C<sub>2</sub> and C<sub>1</sub> increases obviously. However, a large number of C<sub>2</sub> and C<sub>1</sub> in condensate not only increase the difficulty of product separation, but also increase energy consumption.

### 5.2. Parameter sensitivity analysis of equipment

Based on the sequential-modular method, the parameter sensitivity of equipment analysis results are as follows:

- (1) Outlet pressure of expander

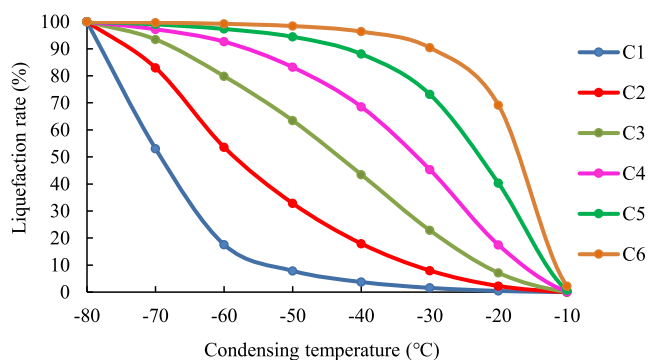


Fig. 6. Liquefaction rate curve of each component of gas in the pressure of 5.0 MPa.

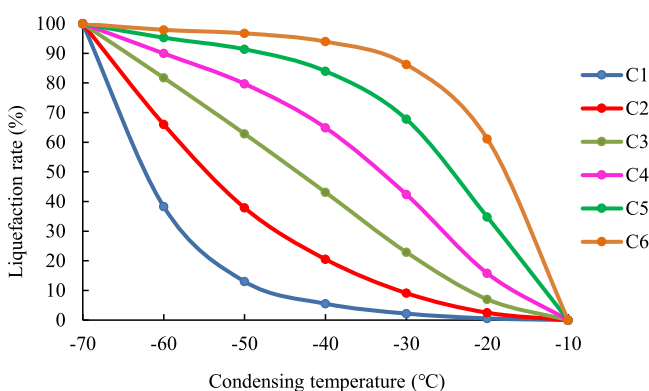


Fig. 7. Liquefaction rate curve of each component of gas in the pressure of 6.0 MPa.

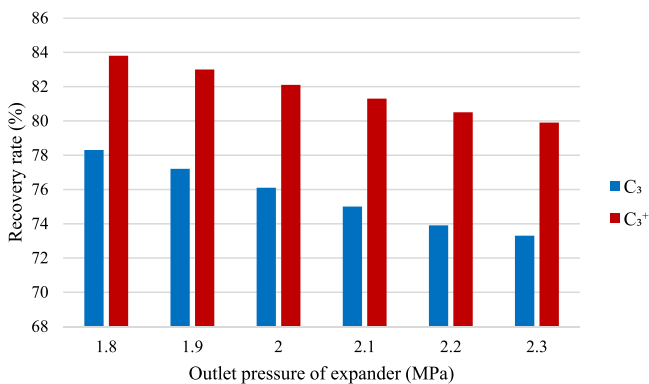


Fig. 8. Change of recovery of  $C_3$  and  $C_{3+}$  with expander outlet pressure.

When the inlet pressure of the expander is 5.96 MPa, the initial value of outlet pressure is 1.8 MPa, and 0.2 MPa is the step length. The influence of expander outlet pressure on the recovery rate of  $C_3$  and  $C_{3+}$  is analyzed in the range of 1.8–2.3 MPa. The effect of expander outlet pressure on recovery of  $C_3$  and  $C_{3+}$  can be seen in Fig. 8, the influence of the expander outlet pressure on the equipment energy consumption is shown in Fig. 9.

It can be seen from Fig. 8 that the decrease of the outlet pressure of the expander has a significant effect on the recoveries of  $C_3$  and  $C_{3+}$ . The lower the outlet pressure of the expander, the larger the expansion ratio, so the lower the temperature of natural gas expanded by the expander, the higher the  $C_3$  and  $C_{3+}$  recovery rate.

It can be seen from Fig. 9, the pressure from 2.2 MPa down to 2.0 MPa, the corresponding energy consumption increased from

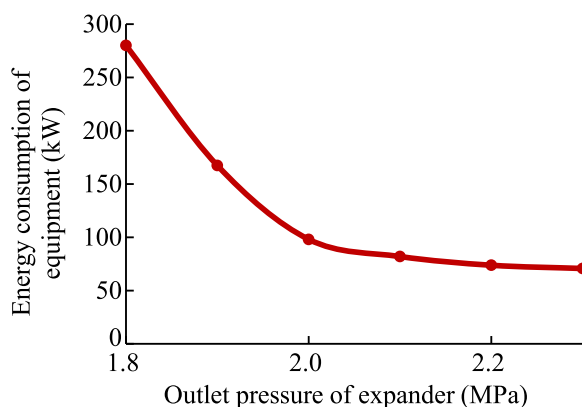


Fig. 9. Change of equipment energy consumption with expander outlet pressure.

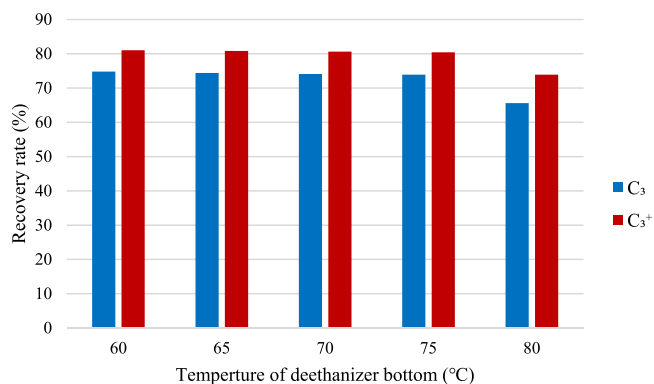


Fig. 10. Change of recovery of  $C_3$  and  $C_{3+}$  with deethanizer bottom temperature.

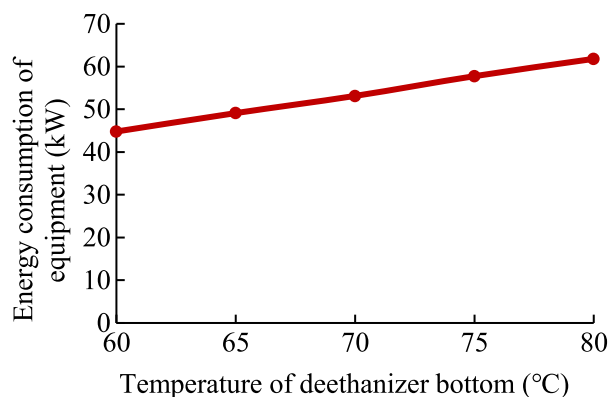


Fig. 11. Change of equipment energy consumption with deethanizer bottom temperature.

73.72 kW to 98.08 kW, an increase of 24.36 kW. When the pressure dropped from 2.0 MPa to 1.8 MPa, the corresponding energy consumption increased from 98.08 kW to 280 kW, an increase of 181.92 kW, indicating that if the pressure drops below 2.0 MPa, the impact of pressure on energy consumption becomes more apparent. Therefore, under the condition of only changing the optimization parameters, it is suggested that the outlet pressure of the expander should be between 2.2 MPa and 2.0 MPa.

(2) Temperature of deethanizer bottom

When the pressure of deethanizer is 2.2 MPa, the initial temperature of deethanizer bottom is 60 °C, and 5 °C is the step length. The influence of deethanizer bottom temperature on the recovery rate of  $C_3$  and  $C_{3+}$  is analyzed in the range of 60–80 °C.

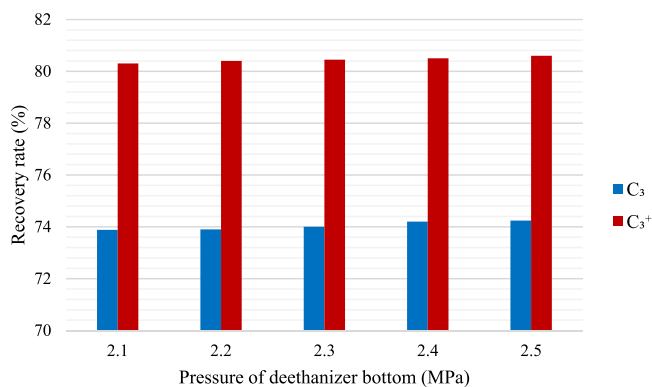


Fig. 12. Change of recovery of C<sub>3</sub> and C<sub>3+</sub> with deethanizer bottom pressure.

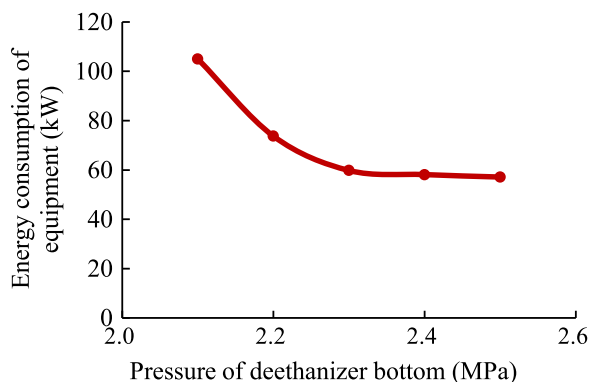


Fig. 13. Change of equipment energy consumption with deethanizer bottom pressure.

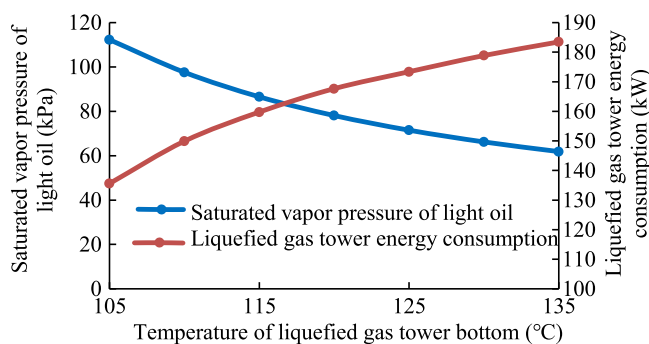


Fig. 14. Change of the saturated vapor pressure of light oil and liquefied gas tower energy consumption with liquefied gas tower bottom.

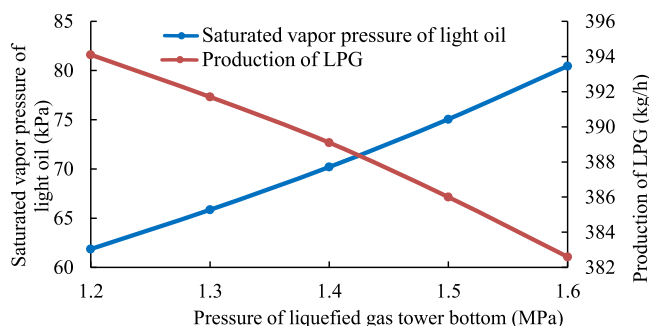


Fig. 15. Change of saturated vapor pressure of light oil and production of LPG with liquefied gas tower bottom pressure.

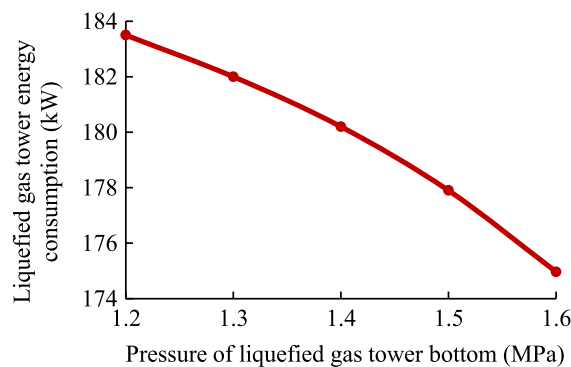


Fig. 16. Change of tower energy consumption with liquefied gas tower bottom pressure.

The effect of deethanizer bottom temperature on recovery of C<sub>3</sub> and C<sub>3+</sub> can be seen in Fig. 10, the influence of the deethanizer bottom temperature on the energy consumption of the device is shown in Fig. 11.

It can be seen from Fig. 10, the recovery rate of C<sub>3</sub> and C<sub>3+</sub> decreases slowly with the increase of the temperature of the deethanizer bottom. This is due to the increase in the temperature of the deethanizer bottom, C<sub>2+</sub> in the top of the tower increases and C<sub>3+</sub> in the bottom of the tower decreases, thus reducing the recovery of C<sub>3</sub> and C<sub>3+</sub>. It can be seen from Fig. 11, the higher the temperature of the deethanizer bottom is, the higher the energy consumption required for the deethanizer reboiler, so the energy consumption of the whole equipment is also increased accordingly.

### (3) Pressure of deethanizer bottom

Keep the bottom temperature of the deethanizer (78 °C) and the top pressure (2.20 MPa) of the deethanizer to be constant. The initial pressure of deethanizer bottom is 2.1 MPa, and 0.1 MPa is the step length. The influence of deethanizer bottom pressure on the recovery rate of C<sub>3</sub> and C<sub>3+</sub> is analyzed in the range of 2.1–2.5 MPa. The effect of deethanizer bottom pressure on recovery of C<sub>3</sub> and C<sub>3+</sub> can be seen in Fig. 12, the influence of the deethanizer bottom pressure on the energy consumption of the device is shown in Fig. 13.

It can be seen from Fig. 12, the recovery rates of C<sub>3</sub> and C<sub>3+</sub> increase slowly with the increase of the pressure of the deethanizer bottom. This is because the pressure of the deethanizer bottom is large, the relative volatilization of the components is reduced, and the C<sub>3+</sub> at the bottom of the deethanizer is not easy to volatilize. However, when the pressure varies slightly (less than 30%), the effect of relative volatility cannot be considered. So the influence of the deethanizer bottom pressure on the recovery rate is less. But increasing the deethanizer bottom pressure will reduce the content of C<sub>2</sub> and C<sub>1</sub> in the top of the deethanizer, and the separation effect will be worse, and the quality of the subsequent products will be affected. It can be seen from Fig. 13, with the increase of the pressure of the deethanizer bottom, the energy consumption of the reboiler at the bottom of the deethanizer is also increased, so the energy consumption of the whole equipment is also increased accordingly.

### (4) Temperature of liquefied gas tower bottom

Keep the operating pressure (1.2 MPa) of the liquefied gas tower to be constant. The initial temperature of liquefied gas tower bottom is 105 °C, and 5 °C is the step length. The influence of liquefied gas tower bottom temperature on the saturated vapor pressure of light oil and liquefied gas tower energy consumption are analyzed in the range of 105 °C–135 °C, as shown in Fig. 14.

It can be seen from Fig. 14, with the decrease of the bottom temperature of the tower, the saturated vapor pressure of light

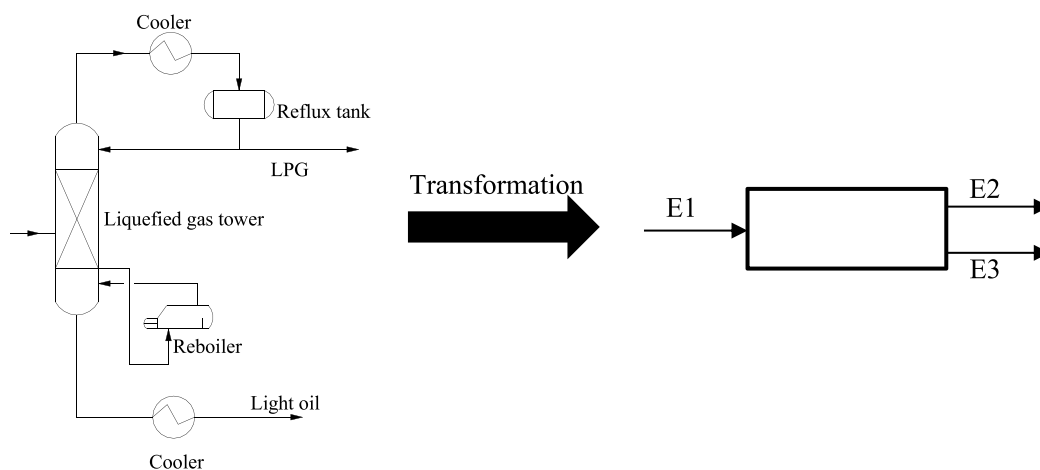


Fig. 17. Black box model of light hydrocarbon recovery system.

**Table 2**  
Exergy loss calculation results for each equipment.

Item		Exergy loss (kJ/h)	Exergy efficiency (%)
Molecular sieve drying system		9888	74.69
Cold box		74 705	91.66
Throttle valve		646	99.56
Turboexpander system	Expander	13 443	98.03
	Compressor	6971	96.32
Deethanizer system	Condenser (Top of tower)	7830	83.49
	Deethanizer	351 141	36.43
	Reboiler (Bottom of tower)	417 557	23.03
Liquefied gas tower system	Condenser (Top of tower)	86 623	77.04
	Liquefied gas tower	73 629	84.16
	Reboiler (Bottom of tower)	52 930	89.63
Overall system		1 095 363	–

**Table 3**  
Optimization calculation results.

Number	1	2	3	4	5
Outlet pressure of expander (MPa)	2.20	2.15	2.10	2.05	2.00
Deethanizer bottom temperature (°C)	78	76	74	72	70
Recovery rate of C <sub>3</sub> (%)	73.9	74.5	75.1	75.7	76.3
Recovery rate of C <sub>3+</sub> (%)	80.6	81.1	81.5	81.9	82.1
Energy consumption of C <sub>3+</sub> (10 <sup>4</sup> kJ/kmol)	172.9	157.9	152.6	150.5	146.8

oil increases and the energy consumption of the liquefied gas tower decreases. For every 1 °C decrease in tower bottom temperature, the energy consumption of the liquefied gas tower will be reduced by 1.5 kW, indicating that the liquefied gas tower bottom temperature has little effect on the energy consumption of the tower. When the temperature of bottom tower is reduced to 120 °C, the saturated vapor pressure of light oil is 78.11 kPa (> 74 kPa), which has reached the requirement. However, the continuous lowering of temperature is not easy for C<sub>3</sub> and C<sub>4</sub> to volatilize in the condensate of the tower bottom, which will affect the quality of LPG.

##### (5) Pressure of liquefied gas tower bottom

Keep the temperature (135 °C) of liquefied gas tower bottom to be constant. The initial pressure of liquefied gas tower bottom is 1.2 MPa, and 0.1 MPa is the step length. The influence of liquefied gas tower bottom pressure on the saturated vapor pressure of light oil and production of LPG are analyzed in the range of 1.2–1.6 MPa, as shown in Fig. 15. The effect of liquefied gas tower bottom pressure on the tower energy consumption can be seen Fig. 16.

It can be seen from Fig. 15, as the pressure at the bottom of the tower increases, saturated vapor pressure of light oil increases, but production of LPG decreases. Therefore, under the condition that the saturated vapor pressure is satisfied, the bottom pressure of the tower should be reduced as much as possible. It can be seen from Fig. 16, as the pressure at the tower bottom increases, the energy consumption of the liquefied gas tower decreases. For every 0.1 MPa increase in liquefied gas tower bottom, the energy consumption of the liquefied gas tower will be reduced by an average of 2.1 kW, which indicates that the pressure of liquefied gas tower bottom has little effect on the energy consumption of the tower.

### 5.3. Exergy analysis results

The black-box model is used to perform exergy analysis of the light hydrocarbon recovery system, treating each device in the system as a black-box model, as shown in Fig. 17. The environmental benchmark pressure is 0.101 MPa, and the benchmark temperature is 25 °C.

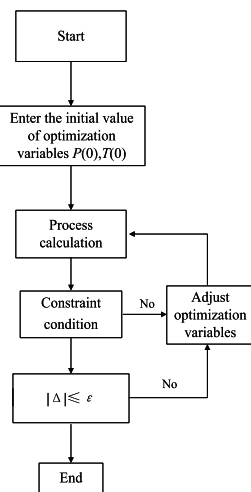


Fig. 18. Optimization flow chart.

The calculation results of exergy can be seen in Table 2. It is known from Table 2 that the exergy loss of the deethanizer system is the greatest. In terms of the exergy efficiency of the single equipment, the reboiler in the deethanizer system has a lower exergy efficiency of only 23.03%. Therefore, when the parameters are optimized, the reboiler load should be reduced as much as possible when the  $C_{3+}$  of deethanizer bottom meets the requirements.

## 6. Optimization of light hydrocarbon recovery system

In the optimization of chemical system, there are usually two ways: one is to adjust the operating parameters of the equipment, the other is to reform the process. Therefore, this section

optimizes the light hydrocarbon recovery system from these two aspects.

### 6.1. Parameter optimization

#### (1) Optimization target

The light hydrocarbon recovery system in DLB condensate field adopts cryogenic separation process by using turboexpander, the main purpose of the system is to increase the recovery rate of  $C_{3+}$ , and improving the recovery rate of  $C_{3+}$  can increase the production of LPG and light oil. However, increasing the recovery of light hydrocarbons will be constrained by the energy consumption of the equipment. Thus, if the maximum recovery rate of light hydrocarbons or the lowest energy consumption is the optimization goal, the maximum total income cannot be guaranteed. Therefore, in this paper, the minimum ratio of total system energy consumption and  $C_{3+}$  recovery is the optimal target, which reflects the lowest cost of recovery of  $C_{3+}$ . The objective function is:

$$F = \min \frac{\sum_i^n E_i}{F_{C_{3+}}} = f(P, T) \quad (19)$$

#### (2) Optimization variables

The optimization variables are composed of two parts: decision variables and state variables. To optimize the operation parameters of the system, the decision variables can be adjusted according to the actual conditions, so it is also called adjustable variables. The selection of system optimization variables should be selected from adjustable variables.

Based on the parameter sensitivity analysis of equipment, outlet pressure of expander and temperature of deethanizer bottom have great influences on the energy consumption of equipment and recovery rate of  $C_3$  and  $C_{3+}$ . Therefore, this paper takes outlet pressure of expander and temperature of deethanizer bottom as optimization variables.

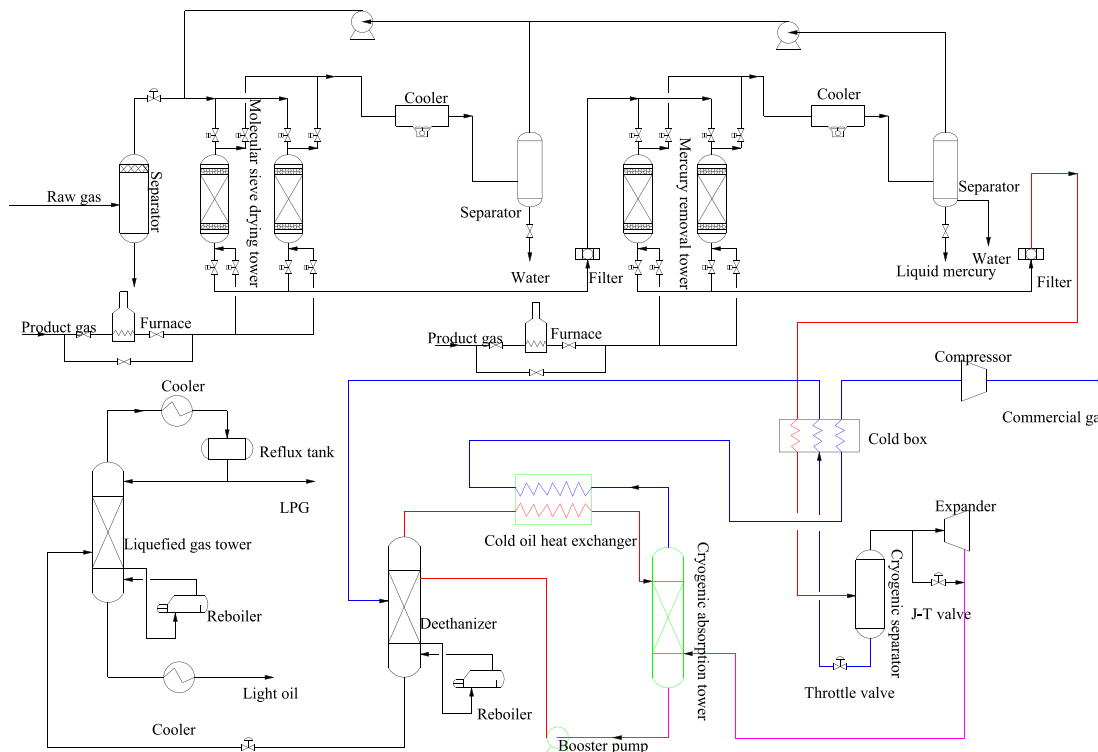


Fig. 19. Process flow of the optimized light hydrocarbon recovery system.

**Table 4**

Optimized parameters of main equipment.

Equipment	Temperature (°C)	Pressure (MPa)
Cryogenic separator	−33	–
Outlet of expander	−72	2.0
Deethanizer bottom	70	2.0
Deethanizer top	−67	2.0
Liquefied gas tower bottom	135	1.2
Liquefied gas tower top	54	1.2

**Table 5**

Main parameters of the equipment in the optimized system.

Equipment	Temperature (°C)	Pressure (MPa)
Cryogenic separator	−33	–
Outlet of expander	−70	2.4
Cryogenic absorption tower bottom	−70	2.4
Cryogenic absorption tower top	−70	2.4
Deethanizer bottom	78	2.53
Deethanizer top	−24	2.52
Liquefied gas tower bottom	135	1.5
Liquefied gas tower top	47	1.5

(3) Constraint condition

$$\left\{ \begin{array}{l} \Delta t = 3 \\ \frac{F_{C_{2-}}}{F_{LPG}} \leq 5\% \\ \frac{F_{C_{5+}}}{F_{LPG}} \leq 3\% \\ 2.0 \leq P \leq 2.2 \\ T \leq 75 \\ 74 \leq P_{sv} \leq 200 \\ P_1 \geq P_C \\ T_1 \leq T_C \end{array} \right.$$

(5) Solution procedure

In this paper, SQP is used to solve mathematical optimization model of light hydrocarbon recovery system. The SQP method is one of the most effective ways to solve the equality and inequality constraints.

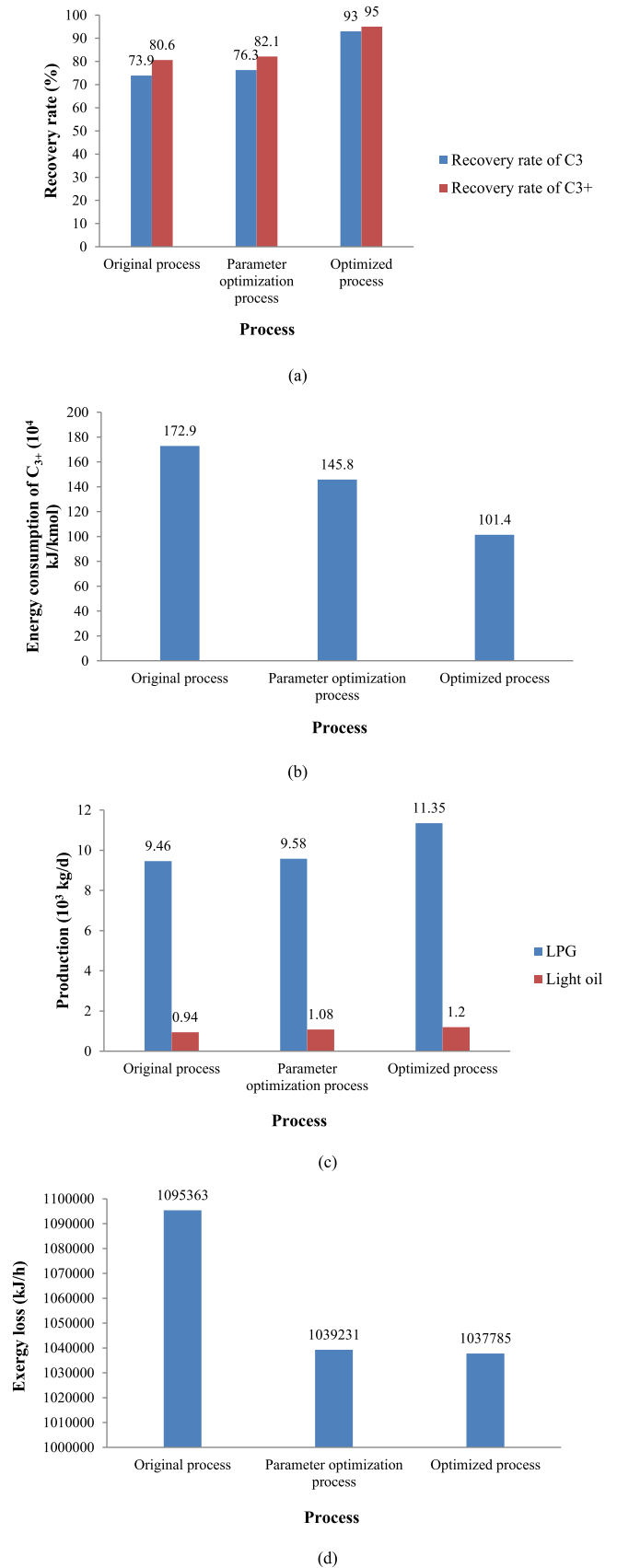
The optimization calculation is an iterative process which is gradually approaching to the optimization target, and the optimization target calculation process is shown in Fig. 18. The influence of optimization parameters on the system recovery rate and energy consumption shows that decreasing the outlet pressure of the expander and decreasing the temperature of the deethanizer bottom can make the objective function change to the optimal goal. When two variables are changed at the same time, there is a set of optimal variable values that make the optimal target value minimum.

(6) Optimization results

The HYSYS software is used to do optimization calculation. The results are shown in Table 3. As can be seen from Table 3, the optimization target has a minimum value (the outlet pressure of the expander is 2.0 MPa, the deethanizer bottom temperature is 70 °C). The optimized parameters of main equipment are shown in Table 4.

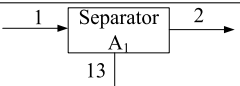
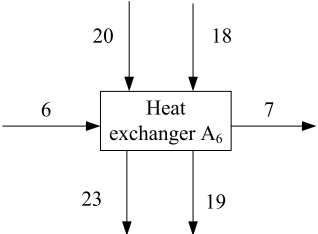
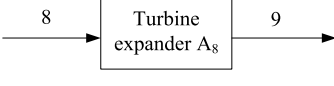
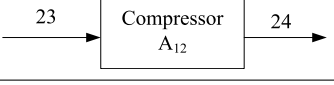
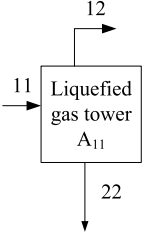
6.2. Process optimization

This paper put forward a reform plan of light hydrocarbon recovery process in DLB condensate field. The DHX technology



**Fig. 20.** Optimization effect evaluation results for different process: (a) recovery rates of C<sub>3</sub> and C<sub>3+</sub>; (b) energy consumption of C<sub>3+</sub>; (c) production of LPG and light oil; (d) energy loss.

**Table A.1**  
Mathematical model of equipment.

Equipment	Structural unit	Required model
Separator		$F_1x_{1,j} = F_2x_{2,j} + F_{13}x_{13,j}$ $x_{2,j} = K_jx_{13,j}$
Heat exchanger		$Q_i = K_iA_i\Delta t_{mi}$ $Q = \sum_{i=1}^2 Q_i = (H_{19} - H_{18}) + (H_{23} - H_{20})$ $= (H_7 - H_6)$
Turbine expander		$S_8 = S_9$ $T_9 = T_8 \left( \frac{P_9}{P_8} \right)^{\frac{k-1}{k}}$ $W = W_s\eta_s$
Compressor		$T_{24} = T_{23}\varepsilon^{\frac{k-1}{k}}$ $P_{24} = \varepsilon P_{23}$
Rectification tower		$V_{j+1}y_{i,j+1} = L_jx_{i,j} + F_{12}x_{i,12} = 0$ $V_jy_{i,j} + V_Fy_{i,F} = L_{f-1}x_{i,f-1} + F_{12}x_{i,12}$ $V_{j+1}y_{i,j+1} = L_jx_{i,j} - F_{22}x_{i,22} = 0$ $F_{11}z_i = F_{12}x_{i,12} + F_{22}x_{i,22}$ $y_{ij} = K_{ij}x_{ij}$ $\sum_{i=1}^{11} y_{i,j} = \sum_{i=1}^{11} x_{i,j} = 1$ $V_{j+1}H_{j+1} = L_jh_j + F_{12}H_{12} + Q_L = 0$ $V_jH_j + V_FH_F = L_{f-1}h_{f-1} + F_{12}H_{12} + Q_L$ $V_{j+1}H_{j+1} = L_jh_j - F_{20}h_{20} + Q_C$ $F_{11}H = F_{12}H_{12} + F_{22}h_{22} + Q_L - Q_C$ $K_{i,j} = K_{i,j}(T_j, P, x_{i,j}, y_{i,j})$ $H_j = H_j(T_j, P, y_{i,j})$ $h_j = h_j(T_j, P, x_{i,j})$

is adopted because the process is easy to transform the existing expansion refrigeration process and has low investment, the light hydrocarbon recovery rate can be greatly improved under the same conditions. That is, adding a cryogenic absorber between the cryogenic separator and the deethanizer, removing the reflux tank of deethanizer and other equipment, adding a cold oil heat exchanger, and the optimized light hydrocarbon recovery process flow is shown in Fig. 19. The optimized parameters of main equipment are shown in Table 5.

### 6.3. Optimization effect evaluation

In order to evaluate the optimization effect, the two optimized processes (Parameter optimization process and optimized process) are compared with the original process. The contents of the evaluation include: the recovery rates of  $C_3$  and  $C_{3+}$ , energy consumption of  $C_{3+}$ , the production of LPG and light oil, energy loss. The evaluation results can be seen in Fig. 20.

It can be seen from Fig. 20:

(1) The recovery rate of  $C_3$  and  $C_{3+}$  in the parameter optimization process is only increased by 2.4% and 1.55%, while the recovery rate of  $C_3$  and  $C_{3+}$  in the optimized process is increased by 19.1% and 14.4%.

(2) The  $C_{3+}$  energy consumption of the optimized process is saved by 26.3% than the parameter optimization process.

(3) The production of LPG and light oil in the parameter optimization process is not obvious compared with the original process, but the optimized process is more obvious.

(4) Compared with the exergy loss, the parameter optimization process is reduced by 5.1% compared with the original process, while the optimized process is reduced by 5.3%.

Moreover, in this paper, the optimization results are compared with other published papers. Xu optimized the DHX light hydrocarbon recovery process in a gas field, increasing the recovery rate of  $C_3$  from 78% to 81% and decrease the energy consumption by 2.84%. Gong optimized the light hydrocarbon recovery system in a gas field in Xinjiang, China, increasing the recovery rate of  $C_{3+}$  products from 97% to 99%. It can be seen that the optimization scheme proposed in this paper makes the recovery rate of light hydrocarbons more effective.

## 7. Conclusions

This paper aims at the problem of low recovery rate of  $C_3$  and  $C_{3+}$  in light hydrocarbon recovery system during the late development of condensate gas field, takes DLB condensate gas field as a case study, sequential-modular method is used to analyze the sensitivity of the system parameters and the process parameters are optimized by SQP method. Moreover, this paper also optimizes the original process using DHX technology. Finally, two optimized processes are compared from the point of recovery rate of  $C_3$  and  $C_{3+}$ , the energy consumption of  $C_{3+}$ , the production of LPG and light oil, energy loss. The following main conclusions are drawn:

(1) The outlet pressure of expander has a great influence on the light hydrocarbon recovery system. The pressure decreases from 2.3 MPa to 1.8 MPa, the recovery of  $C_3$  increases by 5%, and the recovery of  $C_{3+}$  increases by 3.9%. The temperature of the deethanizer bottom also has a great influence on the light hydrocarbon recovery system. The recovery of  $C_3$  increases by 9.2% and that of  $C_{3+}$  increases by 7.1% when the temperature decreases from 80 °C to 60 °C.

(2) Reducing the expander's outlet pressure will increase the energy consumption of the equipment. From 2.0 MPa to 1.8 MPa will increase the energy consumption by 185.7%, while lowering the temperature of the deethanizer bottom will reduce the energy consumption of the equipment, but the decrease is not significant. The energy consumption of equipment will decrease by 27.5% from 80 °C to 60 °C.

(3) Optimized process using DHX technology has a better optimization effect than the parameter optimization process. The  $C_3$  recovery rate of the process optimization scheme is 16.7% higher than that of the parameter optimization scheme, the  $C_{3+}$  recovery rate is 12.9% higher, and the exergy loss has little difference.

### Declaration of competing interest

The authors declare that they have no known competing financial interests or personal relationships that could have appeared to influence the work reported in this paper.

### Acknowledgment

This article is funded by China Scholarship Council (Grant No. 201708030006).

### Appendix

See Table A.1.

### References

- Aggarwal, V., Singh, S., 2001. Improve NGL recovery. *Hydrocarb. Process.* 80, 41–45.
- Baker, R.W., Wijmans, J.G., Kaschemekat, J.H., 1998. The design of membrane vapor–gas separation systems. *J. Membr. Sci.* 151, 55–62.
- Cao, L.J., 2015. Study on Hydrocarbon Recovery Process Optimizati on Light of DLB Condensate Field (Master's Thesis). Southwest Petroleum University, Chengdu, China.
- Chaiwongsa, P., Wongwises, S., 2008. Experimental study on R-134a refrigeration system using a two-phase ejector as an expansion device. *Appl. Therm. Eng.* 28, 467–477.
- Chan, Y.N.I., Hill, F.B., Wong, Y.W., 1981. Equilibrium theory of a pressure swing adsorption process. *Chem. Eng. Sci.* 36, 243–251.
- Cheng, Q., Gan, Y., Su, W., Liu, Y., Sun, W., Xu, Y., 2017. Research on exergy flow composition and exergy loss mechanisms for waxy crude oil pipeline transport processes. *Energies* 10, 1956.
- Cismondi, M., Mollerup, J., 2005. Development and application of a three-parameter RK-PR equation of state. *Fluid Phase Equilib.* 232, 74–89.
- Fernandes, M.X., Huertas, M.L., Castanho, M.A.R.B., Torre, J.G.D.L., 2000. Conformation and dynamic properties of a saturated hydrocarbon chain confined in a model membrane: a brownian dynamics simulation. *BBA-Biomembranes* 1463, 131–141.
- Hillestad, M., Hertzberg, T., 1986. Dynamic simulation of chemical engineering systems by the sequential modular approach. *Comput. Chem. Eng.* 10, 377–388.
- Khan, S.A., 1985. Expander-gas processing plant converted to boost  $C_3$  recovery at Canada's Judy Creek. *Oil Gas J.* 83, 22.
- Krasae-In, S., Stang, J.H., Neksa, P., 2010. Simulation on a proposed large-scale liquid hydrogen plant using a multi-component refrigerant refrigeration system. *Int. J. Hydrog. Energ.* 35, 12531–12544.
- Limb, D.I., Czarnecki, B.A., 1987. Reflux-exchange process lifts propane recovery at Aussie site. *Oil Gas J.* 85, 50.
- Liu, B., Wang, D.W., 2000. Study on the technology of the condensing separation method applied in light hydrocarbon recovery. *Exp. Pet. Geol.* 22, 392–397.
- Lu, H., Guo, L., Azimi, M., Huang, K., 2019b. Oil and gas 4.0 era: A systematic review and outlook. *Comput. Ind.* 111, 68–90.
- Lu, H., Huang, K., Azimi, M., Guo, L., 2019a. Blockchain technology in the oil and gas industry: A review of applications, opportunities, challenges, and risks. *IEEE Access* 7, 41426–41444.
- Lyu, Q.N., Zhang, W.Z., 2010. Application of vortex temperatures separation technology in natural gas industry. *Nat. Gas Oil* 28, 37–42.
- Ma, X., Mei, X., Wu, W., Wu, X., Zeng, B., 2019. A novel fractional time delayed grey model with grey wolf optimizer and its applications in forecasting the natural gas and coal consumption in chongqing China. *Energy* 178, 487–507.
- Morosuk, T., Tsatsaronis, G., 2008. A new approach to the exergy analysis of absorption refrigeration machines. *Energy* 33, 890–907.
- Patel, N.C., Teja, A.S., 1982. A new cubic equation of state for fluids and fluid mixtures. *Chem. Eng. Sci.* 37, 463–473.
- Pitman, R.N., Hudson, H.M., Wilkinson, J.D., Cuellar, K.T., 1998. Next Generation Processes for NGL/LPG Recovery. Gas Processors Association, Tulsa, OK, USA.
- Shin, B.Y., Jang, S.H., Chung, I.J., Kim, B.S., 1992. Mechanical properties and morphology of polymer blends of poly (ethylene terephthalate) and semiflexible thermotropic liquid crystalline polyesters. *Polym. Eng. Sci.* 32, 73–79.
- Wang, X.K., 2003. Application and analysis of natural gas cryogenic process. *Chem. Eng. Oil Gas* 32, 200–201.
- Wilkinson, J.D., Hudson, H.M., 1982. Turboexpander plant designs can provide high ethane recovery without inlet  $CO_2$ /removal. *Oil Gas J.* 80, 18.
- Wu, M.O., 2013. A Natural Gas Condensate Recovery Plant Process Optimization and Modification Research (Master's Thesis). Southwest Petroleum University, Chengdu, China.
- Zhao, X.H., 2003. The Combined Technology of Light Hydrocarbon Recovery by Shallow Cooling-Oil Absorption Development (Master's Thesis). Harbin Engineering University, Harbin, China.
- Zhao, S., 2013. The significance and technological progress of light hydrocarbon recovery of natural gas. *Guangzhou Chem. Ind.* 41, 32–33.